New Insight into Nanoscale Identification of the Polar Axis Direction in Organic Ferroelectric Films

Sajmohan Mohandas Moolayil, Antonio Da Costa, Jean-Francois Tahon, Vincent Bouad, Arthur Hamieh, Freddy Ponchel, Vincent Ladmiral, Denis Rémiens, Jean-Marc Lefebvre, Rachel Desfeux, et al.

HAL Id: hal-04278730

https://hal.univ-lille.fr/hal-04278730

Submitted on 23 Nov 2023

New insight into nanoscale identification of the polar axis direction in organic ferroelectric films

Sajmohan Mohandas Moolayil[1], Antonio Da Costa[1], Jean-François Tahon[2], Vincent Bouad[2,4], Ahmed Hamieh[2,3], Freddy Ponchel[3], Vincent Ladmiral[4], Denis Rémiens[3], Jean-Marc Lefebvre[2], Rachel Desfeux[1], Sophie Barrau[2*], Anthony Ferri[1*]

[1] Univ. Artois, CNRS, Centrale Lille, Univ. Lille, UMR 8181, Unité de Catalyse et Chimie du Solide (UCCS), F-62300 Lens, France

[2] Univ. Lille, Sciences et Technologies, CNRS, Centrale Lille, INRA, UMR 8207, Unité Matériaux Et Transformations (UMET), F-59655, Villeneuve D'Ascq, France

[3] Univ. Polytechnique Hauts-de-France (UPHF), CNRS, UMR 8520, Institut d'Electronique, de Microélectronique et de Nanotechnologie, Département Opto-Acousto-Electronique (IEMN-DOAE), Site de Valenciennes – UPHF, F-59300, Valenciennes, France

[4] ICGM, Univ Montpellier, CNRS, ENSCM, Montpellier, France

ABSTRACT

Ferroelectric poly(vinylidene fluoride-*co*-trifluoroethylene) [P(VDF-*co*-TrFE)] thin films have been deposited by spin-coating onto $Bi_{0.5}Na_{0.5}TiO_3(BNT)/LNO/SiO_2/Si$ heterostructure. Copolymer microstructure investigated by using Grazing-Incidence Wide-Angle X-ray Diffraction (GIWAXD) and deduced from the (200)/(110) reflections demonstrates that the *b*-axis in P(VDF-*co*-TrFE) orthorhombic unit cell is either in-plane or out-of-plane, depending on the face-on or on the two types of edge-on (called *I* and *II*) lamellar structures locally identified by Atomic Force Microscopy (AFM). For edge-on *I* lamellae regions, the electroactivity is found to be twice as high ($d_{zz}^{eff} \sim -50.3$ pm/V) that measured for both edge-on *II* or face-on crystalline domains, as probed by Piezoresponse Force Microscopy (PFM). This result is directly correlated to the direction of the ferroelectric polarization vector in the P(VDF-*co*-TrFE) orthorhombic cell: larger nanoscale piezoactivity is related to the *b*-axis which lies along the normal to the substrate plane in the case of the edge-on *I* domains. Here, the ability to thoroughly gain access to the as-grown polar axis direction within the edge-on crystal lamellae of the ferroelectric organic layers is evidenced by combining the nanometric resolution of the PFM technique with a statistical approach based on its spectroscopic tool. By gathering information at the nanoscale, two orientations for the polar *b*-axis are identified in edge-on lamellar structures. These findings contribute to a better understanding of the structure-property relationships in P(VDF-*co*-TrFE) films, which is a key issue for the design of future advanced organic electronic devices.

Keywords: Ferroelectric organic, Poly(vinylidene fluoride-*co*-trifluoroethylene), Polar axis, Edge-on lamella, Nanoscale, Piezoresponse Force Microscopy

INTRODUCTION

The growing emphasis on understanding the nanoscale properties, in correlation with the structure and morphology of electroactive polymer materials, has become major scientific concern in recent years. Electroactive organic materials are extensively studied and manipulated to enhance their properties and induce new functionalities for the design of electronic devices such as field effect transistor (FET), transducers and data storage devices.[1,2,3,4] One major candidate among ferroelectric organic materials is poly(vinylidene difluoride) (PVDF) and its derivative copolymer, poly(vinylidene-*co*-trifluoroethylene) P(VDF-*co*-TrFE). Regarding the latter, the low temperature ferroelectric phase presents orthorhombic lattice Cm2m similar to PVDF with extended lattice parameters.[5,6,7,8,9] The copolymer displays all-*trans* chain conformations, denoted as FE (ferroelectric) phase or sometimes β-phase in reference to β-phase of PVDF, as shown in Figure 1a. Indeed, this FE-phase has the planar zigzag all-*trans* (TTTT) conformation, resulting in the CH_2–CF_2 and CHF–CF_2 dipoles lying along the normal direction to the polymer chains backbone and thus generating at the macroscopic scale a maximum and observable electric dipole moment (remnant polarization P_r ~6 µC/cm) along the *b*-axis of the unit cell.[10,11,12,13,14] Such polar fluoropolymers exhibit a negative longitudinal piezoelectric coefficient (d_{zz} ~ –30 pm/V)[13,14], *i.e.* they contract in the direction of an applied electric field, unlike more conventional inorganic ferroelectrics. The physical properties of electroactive P(VDF-*co*-TrFE) polymer generally depend on the structure and organization of crystalline lamellae, which depend in turn on the processing conditions, *e.g.* annealing temperature, applied stress or nature of the solvent used for casting.[2,4,15] Crystallinity improvement of the P(VDF-*co*-TrFE) thin films may be achieved by annealing or heating the film above its Curie transition (around 135°C). Rod-like topographical features are one of the signatures of optimized

crystallinity and ferroelectric response of the films.[16,17] The crystalline lamellae of P(VDF-*co*-TrFE) films grown by different methods have usually an isotropic orientation, generating a lower and non-uniform piezoresponse region.[18] While the negative longitudinal piezoelectric response in the crystalline domains was recently described by Liu *et al*.[19] to be independent of the amorphous regions and of the amorphous-crystalline interface, there is still a debate on the contribution to the piezoelectric response on each component.[20]

The nanoscale piezoelectric/ferroelectric properties of P(VDF-*co*-TrFE) samples have already been studied using the piezoresponse force microscopy (PFM) technique.[17,21,22] In particular, the domain switching dynamic was shown by Zhang *et al*.[23] and Gaynutdinov *et al*.[24] An in-depth study of PFM domain imaging was reported by Sharma *et al*. [[17]], while the enhancement of ferroelectric properties in P(VDF-*co*-TrFE) by nanoconfinement was revealed by Liew *et al*.[25]

In the present study, we focus on the local identification of the copolymer macromolecular chain orientations and the related polarization by using the spectroscopic tool of the PFM technique, *i.e.* the switching spectroscopy PFM (SS-PFM) mode. To the best of our knowledge, although it is well-known that the orientation of the ferroelectric polarization is crucial to induce electroactive properties in such organic fluoropolymers (along the normal direction to the macromolecular chains for optimized properties), no detailed investigation about the accurate polar *b*-axis direction in the orthorhombic P(VDF-*co*-TrFE) unit cell has been conducted at the nanometer scale when considering the specific vertical crystal lamellae. Indeed, while it is known that these vertical domains lead to a significant enhancement of the piezoelectric response[18], there are two distinct types of out-of-plane oriented crystalline lamellae within the P(VDF-*co*-TrFE) copolymer, depending on the orientation of the polarization axis in these domains. It thus becomes crucial to be able to identify both types of edge-on crystal lamellae.

EXPERIMENTAL SECTION

Materials. The commercial (VDF/TrFE 80/20 mol%) P(VDF-*co*-TrFE) copolymer was provided by Piezotech. $(Bi_{0.5}Na_{0.5})TiO_3$(BNT)/$LaNiO_3$(LNO)/SiO_2/Si heterostructure used as ferroelectric substrate was prepared as described below.

Growth of inorganic underlying layers. The LNO film was sputter deposited at room temperature on top of a SiO_2/Si substrate using an RF magnetron sputtering system. It was then annealed at 700°C in air to form a (00*l*)-oriented film acting as a conducting substrate and to improve the electrical conductivity of the film. Details on the manufacturing process and properties of LNO are given elsewhere.[26] BNT layer was also sputtered deposited at 250°C on top of the LNO/SiO_2/Si heterostructure previously fabricated using similar RF magnetron sputtering system. The film is then annealed at 650°C in air to lead to the (00*l*)-oriented ferroelectric film. A detailed description of these BNT films can be found elsewhere.[27] The deposited thickness of LNO and BNT layers are 200 and 350 nm, respectively.

Fabrication of P(VDF-*co*-TrFE) thin films. The P(VDF-*co*-TrFE) films were prepared using the following procedure. 0.5 g of copolymer was dissolved in 10 g of acetone and stirred at ambient temperature until complete solubilization of the copolymer. 400 μL of this solution was then dropped on top of the substrate and spin coated at 2500 rpm for 45 s. The residual solvent was removed by drying the film at 70°C in a vacuum oven for at least 5 h. To finally achieve a complete smooth layer of the copolymer and to lead to self-arranged features on the substrates, we have considered the melt-crystallization process. The films were melted at 180°C for 3 hours

under air, then slowly cooled down with a cooling rate of around 1.25°C/min to room temperature under ambient conditions. A 300-nm-thick copolymer layer was grown.

Characterizations. The structure of the P(VDF-*co*-TrFE) thin films was characterized by the Grazing-Incidence Wide-Angle X-ray Diffraction (GIWAXD). The experiments were carried out using a Xeuss 2.0 (XENOCS) with a GeniX3D micro-source ($\lambda_{Cu} = 1.54$ Å). The sample was put on the specific GIWAXD sample holder and the sample-to-detector distance was 100 mm.

The surface morphology and the roughness of the copolymer films were characterized by the Tapping mode of the Atomic Force Microscopy (TM-AFM) (MultiMode 8-HR, Bruker, USA). To assess the nanoscale piezoelectric properties, the dual AC resonance tracking (DART) method of the PFM mode provided by a commercial AFM microscope (MFP-3D, Asylum Research/Oxford Instruments, USA) was used under environmental conditions. The DART-PFM mode allows for amplifying the detected electromechanical signal by scanning at the contact resonance frequency of the cantilever.[28] By using SS-PFM, piezoresponse hysteresis loops were recorded over the free surface of the polymer films giving access simultaneously to polarization reversal and piezoelectric activity. The loops were measured in remnant mode, where rectangular voltages pulses were applied and the PFM signal was collected at zero field, promoting electromechanical response while minimizing electrostatic contribution. All local piezoelectric measurements were carried out by using Pt/Ir-coated tip and cantilever with a nominal ~3.8 N/m spring constant (PPP-EFM, Nanosensors) as the nanometric conductive probe.

RESULTS AND DISCUSSIONS

The structure of deposited P(VDF-*co*-TrFE) copolymer thin films were finely characterized by WAXD measurements at grazing incidence. The GIWAXD pattern in Figure 2a shows the

presence of one main discontinuous ring indicative of a non-isotropic distribution of the P(VDF-co-TrFE) macromolecular chains on the BNT substrate. Figure 2b represents the integrated intensity profiles of P(VDF-co-TrFE) layer. The diffractogram exhibits one main peak at $2\theta = 19.95°$ corresponding to the (200)/(110) planes and attributed to the polar P(VDF-co-TrFE) crystal phase.[29] The calculated interplanar distances are related to an orthorhombic unit cell with the following parameters: $a = 0.890$ nm, $b = 0.505$ nm and $c = 0.255$ nm,[30,31] the macromolecular chains being along the c-axis and the polarization direction oriented along the b-axis.[32] It should be noted that the two (200) and (110) orientations cannot be differentiated by GIWAXD measurements due to similar interplanar distances (see Figure 1b).

As reported by Bargain et al.,[33] a fraction of defective ferroelectric (DFE) phase comprising conformational defects including gauche conformations contributes to a shoulder on the copolymer main diffraction peak. The GIWAXD spectra were then fitted by a pseudo-Voigt function in order to estimate the degree of crystallinity (χ) and the fraction (F) of the ferroelectric (FE) and DFE crystal phases from the ratio of their respective peak area contribution to the total crystal peak area. The peak associated to the DFE is observed at $2\theta = 18.6°$. The crystallinity degree calculated for the copolymer is around $\chi = 70\%$ with a fraction $F_{FE} = 55\%$ and $F_{DFE} = 14\%$ for the copolymer. Depending upon the different defects present in the P(VDF-co-TrFE) the d-spacing along a- and b-axis of the orthorhombic unit cell increases and the peak position shifts to the lower 2θ values. In addition, Spampinato et al.[34] reported three different DFE phases existing in the copolymer with respect to the amount of defects.

Figure 3a represents the evolution of the main peak intensity at $2\theta = 19.95°$ with the azimuthal angle (ϕ) from 0° to 180°. The intensity is maximum at $\phi = 25°$ and 160° suggesting the tilt of the d-spacings d_{200}/d_{110} at the same angle. Considering the (200) reflections in the orthorhombic

unit cell, the *a*-crystallographic axis presents an angle of ±20-25° and the *b*-axis lays parallel to the substrate plane, respectively. In the case of the (110) reflections, the *a*-crystallographic axis presents an angle slightly lower than ±20-25° while the *b*-axis lays quasi-parallel to the substrate plane.

A maximum with a lower intensity is observed at $\phi = 90°$. In this case, for the (200) reflection in the orthorhombic unit cell, the *a* and *b* crystallographic axes lay perpendicular and parallel to the substrate plane, respectively, while for the (110) reflection, the *a* and *b* axes present an angle of 30 and 60° with the substrate plane, respectively.[35] These oriented orthorhombic unit cells with respect to the plane of the BNT substrate are shown on Figure 3b. The macromolecular chains are then laid along to the substrate implying a fraction of the crystalline lamellae oriented in a direction perpendicular to the substrate (so-called edge-on lamellar structure). These various orientations for the crystal lamellae are illustrated in Figure 3c.

AFM surface morphology

Figure 4 represents the TM-AFM topography of the P(VDF-*co*-TrFE) thin film. These AFM images give access to the direct visualization of the microstructure of the melt-crystallized copolymer correlated to the macromolecular chain arrangement. As seen in Figure 4a, the P(VDF-*co*-TrFE) layer deposited onto BNT film displays a complex morphology, leading to a high RMS roughness of ~ 41.0 nm. Horizontal crystalline domains appearing as irregular flakes coexist with perpendicular arranged lamellae showing particular needle-shaped, leading to the generation of many interfaces. Very similar AFM morphology was reported for P(VDF-*co*-TrFE) film deposited onto silicon substrate.[36] This result is also in correlation with the previously described GIWAXD analyses (Figure 2), where the crystalline lamellae were found to be in-

plane (IP) and out-of-plane (OP) oriented, related to well-known face-on and edge-on crystals in such semi-crystalline polymers (see Figure 3c). By further analyzing the surface morphology over the whole surface of the sample, two well-defined kinds of microstructures are clearly evidenced, corresponding to horizontal (face-on) and perpendicular (edge-on) lamellae regions. Figure 4b highlights the specific face-on zone, where a horizontal growth of the crystalline lamellae leads to the IP stacking of lamellae, forming steps. The curve profile of the AFM topography associated to the green dotted line and shown in Figure 4e reveals a height of around 20 nm for the stacking layers. This value corresponds to the domain periodicity, including crystalline lamella and amorphous region existing in-between two lamellae, and called the long period. The obtained values are in agreement with the value of the long period typically found in semi-crystalline polymers, *i.e.* of the order of a few tens of nm.[33,37] Figure 4c represents the detailed morphology of domains formed by perpendicular lamellae structure, called edge-on *I* lamellar structure hereafter. The lamellae are periodically stacked together along the *c*-axis of the orthorhombic cell of the P(VDF-*co*-TrFE) and separated by the amorphous phase, leading to perpendicular arranged structures. The lamellae thickness ranges from 140 nm up to 180 nm, as depicted in the height profile in Figure 4f. Such large values of lamellar thickness (>100 nm) have already been reported for fluorinated polymers.[38] Considering that in the present case non-isothermal crystallization occurs with a fairly large residence time between the melt and the Curie transition temperatures, chain extended crystallization process may occur as postulated in [16,39,40]. In addition, we observe another type of morphology for edge-on lamellae, called edge-on *II* in this study, as seen on Figure 4d. In this case, the lamellae are periodically stacked together but perpendicularly to the longitudinal axis seen in the AFM image. The thickness of these

stacking arrangements (including both crystalline structures and amorphous regions) ranges from 40 nm up to 120 nm, as shown in the associated height profile in Figure 4g.

Such inhomogeneous surface morphology was already observed in the literature for P(VDF-co-TrFE) films, depending on various elaboration parameters (thin film fabrication processes, pressure, annealing temperature, thickness or substrate nature, …)[7,17,21,2521,3636,41,42,43,44,45], and is in perfect agreement with the GIWAXD experiments described above. From application perspectives such as nanodevices, the high roughness associated to the heterogeneity of the crystalline morphology is an important limitation. Indeed, the control of the polarization is difficult due to the non-uniform local fields[41,46] as we will show afterwards in the case of the domain manipulation by PFM lithography experiments. Nevertheless, in the context of the present study, such a complex surface morphology is essential.

Poling experiments

The electroactive properties of the PVDF-based copolymer deposited were then investigated at the *sub*-micrometer scale by locally manipulating the ferroelectric domains *via* the conductive probing tip of the AFM instrument. Poling experiments were carried out using PFM lithography with DC voltages of ±70 V applied to the AFM tip when scanning square areas at the free surface of the films (the DC voltages were intentionally set at these values in order to overcome the polarizing voltage coercivities deduced from local piezoresponse loops shown afterwards, usually allowing for efficient polarization reversal in both samples). The recorded OP-PFM phase and amplitude responses are shown on Figure 5b,c as well as the corresponding AFM topographic image in Figure 5a. Besides, the sequences of the applied DC voltages are specified on the PFM phase pattern (Figure 5b). Clear inverted contrasts are observed from the phase

signal (Figure 5b) which are associated to the domains with upward and downward polarization for bright and dark regions, respectively. These signals suggest the effective switching of the ferroelectric polarization within the polar phase of the grown copolymers originating from the rotation of the permanent dipoles around the macromolecular chains and the movement of domain walls. This result is further confirmed by the profile curve of the PFM phase signal on Figure 5d corresponding to the dashed blue line seen in Figure 5b where 180° for phase difference of polarized regions is displayed. Simultaneously recorded OP-PFM amplitude images presented on Figure 5c exhibit strong piezoelectric deformation for the two inversely poled regions, as revealed by the bright contrasts measured on the polymer film. Uniform amplitude contrasts are observed on the P(VDF-*co*-TrFE)/BNT sample for the two types of artificially OP-oriented domains signifying a homogeneous electromechanical behavior. Thin dark boundaries are seen on the OP-PFM amplitude image, attributed to the domain separating two opposite polarized domains where the PFM signal falls due to the change of polarization. These boundaries are highlighted in Figure 5e where the profile curve associated to the dashed green line seen in Figure 5c is shown (blue arrows indicate the amplitude sharply dropping at the created domain walls). In addition, no change in the morphological properties is noticed after the polarizing process, as revealed on the simultaneously recorded AFM image in Figure 5a, attesting that the detected PFM contrasts are exclusively due to the electroactive properties of the PVDF-based copolymer. It is worth noting that uniform OP-PFM phase and amplitude contrasts observed for the copolymer may also agree with the existence of edge-on structure lamellae in which the polarization reversal is more effective owing to the rotation of the dipoles about the *c*-axis upon normal electric field and for which the ferroelectric retention properties are superior.[47] It should be noted that although the thermal conditions employed in the present study are not

ideal for achieving optimized piezoelectric performances in P(VDF-*co*-TrFE), the quality of domain switching related to the –CF$_2$– dipole moments rotation along the poling direction is definitively shown. Indeed, a relatively high degree of polarization alignment is obtained in the manipulated areas.

In addition, we notice that some artificially switched regions were grown beyond the AFM tip writing areas, as marked by the white arrows on the Figure 5b, which can be explained by the domain flow process under the high tip electric fields[48] and can further provide an insight in the degree of non-uniformity in the local switching potential previously mentioned.[46] Furthermore, a particular behavior is observed for the edge-on lamellae structures. The electrical bias-induced polarization orientation within these vertical lamellae during PFM lithography process propagates beyond the scanned area by several micrometers. This phenomenon is particularly highlighted by the white dotted squares and the corresponding insets in Figure 5a,b,c. Bright contrasts for vibration amplitude response as well as for phase signal related to the upwards polarization are clearly visible compared to as-grown (not manipulated) dark regions. This direction of the polar vector well agrees with the surrounded positively polarized regions. The extension of the imposed orientation for the edge-on crystals may again be mainly explained by the domain flow process already reported by Hu *et al*.[48]**Erreur ! Signet non défini.** This phenomenon has already been observed in PVDF copolymer films,[41] where the authors showed that this large extension of ferroelectric signal could be controlled by nanoconfinement. Besides, higher PFM response as well as better ferroelectric retention properties were reported for similar edge-on oriented crystals.[7]

Piezoloop measurements

To get more precise information about electroactive behavior of the P(VDF-*co*-TrFE) crystalline domains, the local polarization reversal and electromechanical activity were then probed over the free surface of the sample by using the SS-PFM tool. The conductive AFM tip acting as a nanometric top electrode allows access to the coercive voltage (V_c) and the effective piezoelectric coefficient (d_{zz}^{eff}) associated with the OP component of polarization of the single probed domain. A statistical study was conducted by recording fifty piezoloops over each the different morphologies previously described, *i.e.* on the face-on or edge-on (*I* and *II*) lamellar crystal domains observed for the polymer layer. Figure 6 displays the histograms showing the distribution of the V_c and d_{zz}^{eff} values deduced from the simultaneously measured phase and amplitude piezoloops, respectively. Regardless the type of surface morphology, Gaussian distributions of coercive voltages and amplitude responses are obtained, the average values of which are summarized in Table 1. These PFM signals mainly arise from the crystalline part of the semi-crystalline P(VDF-*co*-TrFE) copolymer. However, knowing the flipping behavior highly depends on the crystallinity degree of the film, we cannot completely exclude the influence of the presence of amorphous regions when probing the domains beneath the AFM tip. Indeed, we previously shown that about 30% of amorphous phase exists in the sample. The V_c values were determined by measuring the half-width of the phase piezoloops, while the d_{zz}^{eff} values were estimated by using the following equation: $A = d_{zz}^{eff} \times V_{ac} \times Q$, where A is the PFM amplitude, V_{ac} is the driving voltage (1.5 V for all measurements) and Q is the quality factor (Q was found to be ranging between 20 and 30 in the experiments, in concordance with the polymeric nature of the material).

Relatively wide distributions for V_c and d_{zz}^{eff} values are obtained. They are centered around 33.8 V and –30.0 pm/V, respectively, for the face-on lamellae regions. For the vertically stacked

lamellae, average values of 36.4 V and –50.3 pm/V for edge-on *I* on the one hand, and 37.4 V

and –27.1 pm/V for edge-on *II* are determined. No significant difference in switching properties

is observed for the three kinds of morphologies observed at the surface of this sample, as shown

by the very similar values of the polarizing voltage coercivity summarized in Table 1. This result

is rather unexpected considering the heterogeneity of the probed crystalline morphology.

Although 180° for phase difference is systematically detected in accordance with the switching

process of the dipole moments, the face-on or edge-on nature does not seem to significantly

impact the average coercive voltages measured, unlike the study reported by Martínez-Tong *et

al*.[41] From the V_c values and based on the 300-nm-thick P(VDF-*co*-TrFE) layers, the coercive

fields can be estimated (even if we have to keep in mind that the electric field seen by the film is

highly inhomogeneous due to the particular contact between the film surface and the nanoscale

geometry of the AFM tip acting as top electrode). They are ranging from 112.7 MV.m^{-1} (V_c =

33.8 V) up to 124.7 MV.m^{-1} (V_c = 37.4 V), higher than usual values reported for bulk PVDF or

copolymers materials (50 MV.m^{-1}).[49,50] These higher energy barriers required for dipole rotation

leading to efficiently flipping of the –CF$_2$– groups around the macromolecular chains (*c*-axis) are

mainly related to the non-optimized crystal quality of the films which are crystallized upon

cooling from melting.

Now, when considering the trend of the piezoelectric response observed over the polymer

surface, it is worth noting that a notably strong piezo-activity is locally detected when probing

the specific edge-on *I* lamellae regions (~ –50.3 pm/V), much higher than for the similarly

vertically-grown lamellae (denoted edge-on *II*) or for the face-on structures. Indeed, in the latter

case the electromechanical responses measured by the AFM tip as well as over the edge-on *II*

structures (–27.1 pm/V) are nearly similar. Consequently, the particular morphological arrangement of the crystalline lamellae described in detail above (Figure 4a,b,c,d) does not seem to be the main parameter to explain such difference in the measured deformation amplitude, even if it should be still pointed out that the observed vertical structures reveal two distinct morphological arrangement of stacked lamellae. In an attempt to explain such a difference in the nanoscale mechanical deformation, the specific orientation for the polymer chains in the P(VDF-co-TrFE) cell has to be considered. The face-on crystal lamellae observed for the organic layer possess their a- and b-axis of the orthorhombic cell in the IP direction, as previously mentioned and confirmed by GIWAXD analysis. In the case of the edge-on I and II lamellae, the c crystallographic axis lies definitively along the substrate plane, but there is no certainty about the exact orientation of the b-axis, $i.e.$ it can be either parallel or oriented at 60° with respect the substrate plane (see Figure 3c). As already mentioned, in the orthorhombic cell of P(VDF-co-TrFE), it is established that the polarization vector is aligned parallel to the b-axis where the remnant polarization is maximized.[25,31] This specific direction allows for a more effective switching of polarization since the ferroelectric dipole moment can easily rotate around the horizontal chain c-axis ($i.e.$ the chain backbone) under application of OP electric field.[18,21,47] In addition, the piezoelectric activity mostly comes from the global dimensional change of the material, which induces modification in the density of dipole moments. This results in ferroelectric polarization change inducing the piezoelectric effect.[13,14,25] As a result, the preferential polar axis orientation directly causes the enhancement of the piezoelectric constant. By assuming the local deformation mainly occurs in the thickness direction, the much higher d_{zz}^{eff} piezoelectric coefficient detected in this work over the edge-on I crystal lamellae can be directly related to the direction of the b crystallographic axis in the P(VDF-co-TrFE)

15

orthorhombic cell, which would have in this case a large component along the normal direction to the substrate plane, same as the ferroelectric polar vector direction. On applying vertical electrical voltage during poling process *via* the AFM tip, the CF_2 molecular dipoles preferentially align along this direction, perpendicular to polymer chain (*c*-axis). In this case, we can state we locally probe the (110)-oriented edge-on lamellae, previously identified as edge-on *I* structures, in which the ferroelectric polarization is inclined at an angle of 60° to the substrate plane (Figure 3c) leading to the strong OP-PFM signal. On the other hand, it is well-established that the local polarization reversal upon OP electric field in such edge-on crystal domains with (110) orientation can occur according three different angles: 180°, 120° and 60° depending on the strength of the applied electric field.[17]

On the contrary, for the lower d_{zz}^{eff}, we can reasonably establish that the *b*-axis in edge-on *II* lamellae would be aligned along the substrate plane, *i.e.* when the polarization vector alignment is not favorable for leading to highest deformation under applied OP driving voltage.[12,18] In this case, the rotation of dipole moments in the direction of applied electrical bias would require to change the alignment of the chain axis. A mechanism where the switching would be possible thanks to the torque on the dipole moment that eventually would enable its rotation was suggested but in any case this would be less effective.[35] This is further supported by the nearly similar polarization reversal and piezoelectric deformations of the face-on structures where the *b*-axis lies definitively along the substrate plane. These cases are attributed to the (200)-oriented edge-on lamellae, previously so-called as edge-on *II*. As a result, whatever the face-on or edge-on orientation, the key parameter to consider in order to fully understand the particular nanoscale electromechanical behavior in such P(VDF-*co*-TrFE) films is the alignment of dipoles, *i.e.* the specific polar *b*-axis direction. The schematic representations of the different molecular chain

orientations for crystalline P(VDF-*co*-TrFE) lamellae with the related polarization axis, with respect to the local piezoelectric deformation detected beneath the AFM tip, are presented in Figure 7. The evidence of the impact of the polar axis orientation in P(VDF-*co*-TrFE) layers on their electrical properties was already extensively reported in the literature[12,24,51], but rarely at such local scale. Lau *et al.* have reported the recording of piezoresponse loops on both face-on and edge-on PVDF copolymer structures, where the coercive voltage was found to be similar and the PFM signal higher in the case of the edge-on crystals.[52] Kim *et al.* and Martínez-Tong *et al.* have also described better local ferroelectric performances of needle crystals by means of PFM technique in the case P(VDF-*co*-TrFE) layers.[7] However, they did not thoroughly discriminate between the two types of edge-on crystalline lamellae since no information on the specific location probed over the film surface is given, thus they did not provide insight on the precise polarization direction. More interesting is the absence of PFM hysteresis loop detected when probing flat-on oriented P(VDF-*co*-TrFE) ultra-thin films and the well-defined PFM loops for the edge-on oriented counterpart, as reported by Wu *et al.*[18] Nevertheless, this latter result reflects only two extreme cases, not taking into account more complex situations in the edge-on oriented crystals. Gutiérrez-Fernández *et al.* have recently highlighted the homogeneous OP polarization reversal attributed to the (110) orientation of the edge-on P(VDF-*co*-TrFE) lamellae when artificially manipulated by PFM lithography, while inhomogeneous OP-PFM phase contrasts were observed for the (100) reflection of the edge-on structures.[35] These latter results clearly show the influence of the polarization vector on the local electromechanical performances of the PVDF-based copolymer. However, they are carried out by manipulating the domains and then by imaging the poled regions, *i.e.* in this case the signal is recorded at the micrometer scale and without any information about the associated surface morphology. Finally, Sharma *et al.*[17]

have reported on the visualization of the polarization distribution in the P(VDF-TrFE) compound using OP- and IP-PFM imaging. In that case, they focused on copolymer nanostructures (*i.e.*, isolated highly crystalline nanomesas with lateral dimensions ranging from 100 to 500 nm and of thickness 3 and 12 monolayers, prepared *via* Langmuir-Blodgett deposition), rather than thick films as in the present study. While their results are of very high quality, our investigation aims to explore both types of edge-on structures, which do not exist in the case of nanomesas.

Therefore, the reported approach enables to gain access to the as-grown polar axis direction within the crystalline structures of the organic layer by taking advantage of the nanometric resolution as well as the very high sensitivity of the spectroscopic PFM tool. More specifically the polar crystallographic axis direction is identified within the well-defined local morphology. In particular, clear assessment of the crystallographic orientation of the edge-on crystal lamellae allows for a better understanding of the structure-property relationship in such electroactive P(VDF-*co*-TrFE) polymers.

CONCLUSIONS

In the present work, we carefully investigated the polar *b*-axis direction in P(VDF-*co*-TrFE) orthorhombic unit cell with respect to the surface of the substrate, when deposited in thin films. Taking advantage of GIWAXD technique for microstructural characterization, AFM for surface morphology analysis, PFM for ferroelectric domains imaging and local piezoresponse loops for measuring switching properties and piezoactivity, we demonstrated the coexistence of regions with the *b*-axis in the plane and out of the plane of the film, as deduced from GIWAXD measurements based on the (200)/(110) planes of reflections. Through AFM images and piezoloops, we deduced than the OP *b*-axis was only found for a fraction of edge-on lamellar

structure, namely edge-on *I*, with the (110) plane parallel to the surface of the film. The other fraction of edge-on lamellar structure, namely edge-on *II*, is characterized by the IP *b*-axis and the (200) planes parallel to the surface of the film. The edge-on *I* lamellar structures display a large d_{zz}^{eff} value of around –50.3 pm/V. In contrast, the edge-on *II* lamellae structures and face-on lamellar structures lead to lower average d_{zz}^{eff} values of –27.1 and –30.0 pm/V, respectively. Such a result highlights robust relationship between structure, surface morphology and electroactivity in P(VDF-*co*-TrFE) layers at the *sub*-micrometer scale, by carefully combining GIWAXD and AFM analyses. In particular, distinct piezoactivity is clearly detected for edge-on lamellar regions. Consequently, these findings are of general interest since they evidence the possibility of accurately identifying the polar axis direction in the case of edge-on crystal lamellae, known for governing the performances of the fluoro-piezopolymers. Thus, improvement of functional properties might be achieved by promoting only edge-on *I* crystalline structures.

AUTHOR INFORMATION

Corresponding Author

*Anthony Ferri, E-mail: anthony.ferri@univ-artois.fr

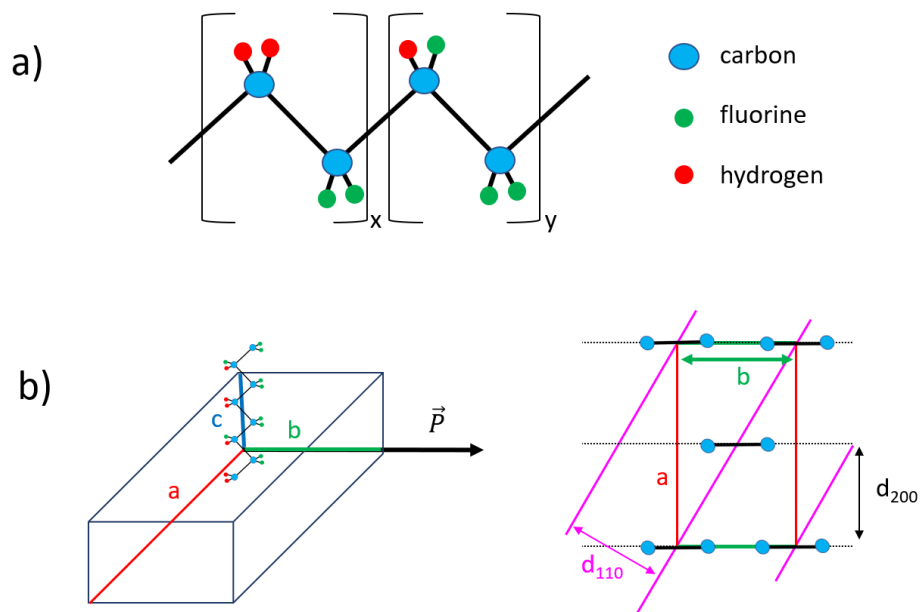*Sophie Barrau, E-mail: sophie.barrau@univ-lille.fr

Figure 1. Schematic representations of the (a) P(VDF-*co*-TrFE) repeat units and the (b) orthorhombic crystal cell with the polar axis along the *b*-axis direction.
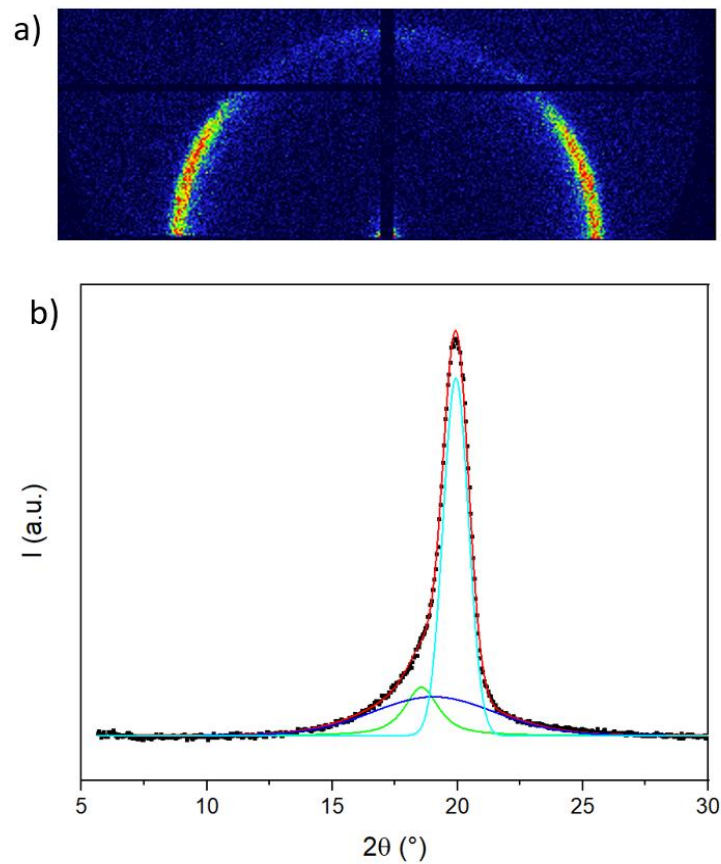
Figure 2. (a) GIWAXD pattern and (b) integrated intensity profiles for P(VDF-*co*-TrFE) film with deconvoluted peaks corresponding to the ferroelectric (FE) phase in cyan, to the defective ferroelectric (DFE) phase in green and to the amorphous contribution in blue.
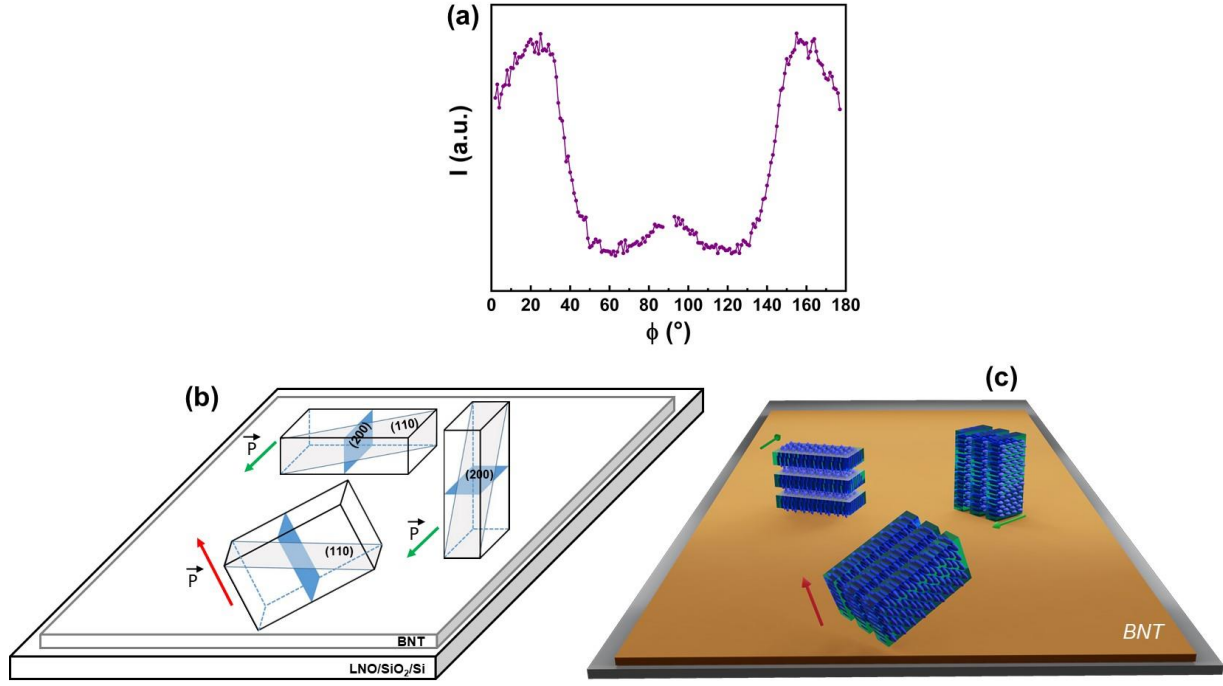
Figure 3. (a) Intensity evolution of (200)/(110) main peak with azimuthal angle for P(VDF-*co*-TrFE) layer. (b) Schematic illustration of the possible orientations of the P(VDF-*co*-TrFE) orthorhombic unit cell with respect to the surface planes of BNT/LNO substrate. The P(VDF-*co*-TrFE) orthorhombic unit cells with the ±20-25° tilted (200)-plane and the ±20-25° tilted (110)-plane with respect to the normal of BNT surface planes [(cases of Figures b)], have not been represented for the sake of clarity. Green (in-plane) and red (out-of-plane) arrows represent the polarization vector along the *b*-axis in the various oriented orthorhombic unit cells of the copolymer. (c) Schematic illustration of the face-on and edge-on crystal lamellae of P(VDF-*co*-TrFE) polymer.
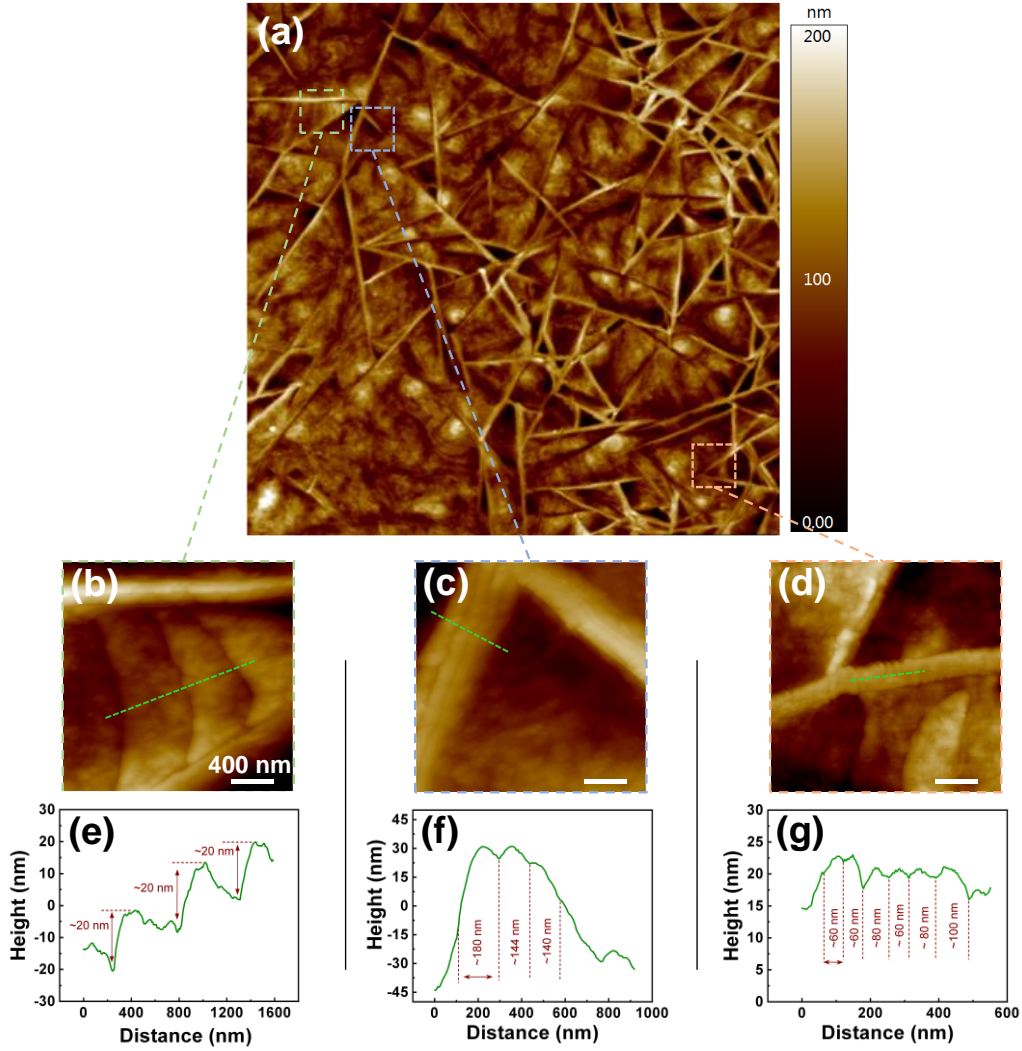
23

Figure 4. AFM surface morphology of the grown P(VDF-*co*-TrFE) layer. (a) Large (60×60 μm²) topographic image of the P(VDF-*co*-TrFE) surface. Enlarged images of the three different morphologies observed at the surface of the polymer marked with dotted squares: (b) horizontal (face-on), (c) vertical (edge-on *I*) and (d) vertical (edge-on *II*) lamellar structures. The height profiles in (e), (f) and (g) below each enlarged AFM images corresponds to the dashed green lines.
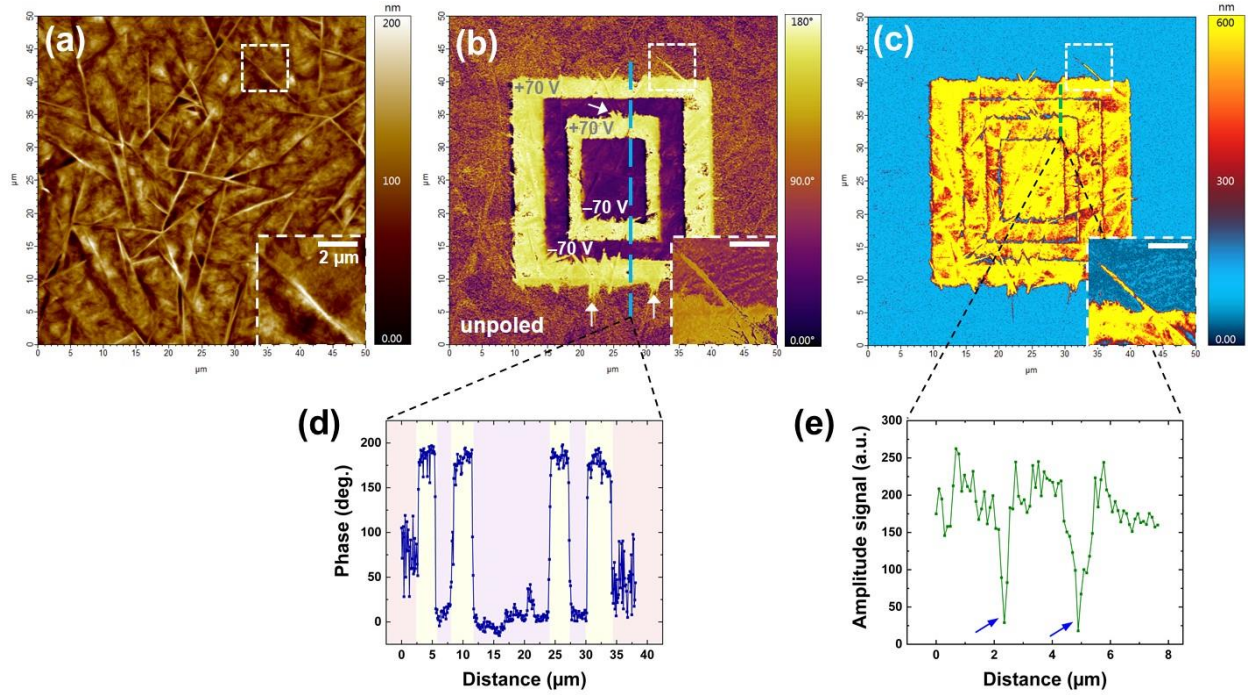
Figure 5. Local manipulation of the polarization direction in the P(VDF-*co*-TrFE) layer. (a) AFM topography, (b) OP-PFM phase and (c) OP-PFM amplitude images simultaneously recorded after applying ±70 V to induce polarization reversal within the electroactive polymer. Insets in the bottom right corner of the images are the enlarged images of the corresponding areas marked with white dashes, displaying unusual electromechanical behavior for edge-on crystals. Profile curves of the PFM phase signal corresponding to the dashed blue line seen in (b) and PFM amplitude signal associated to the dashed green line seen in (c) are shown in (d) and (e), respectively.
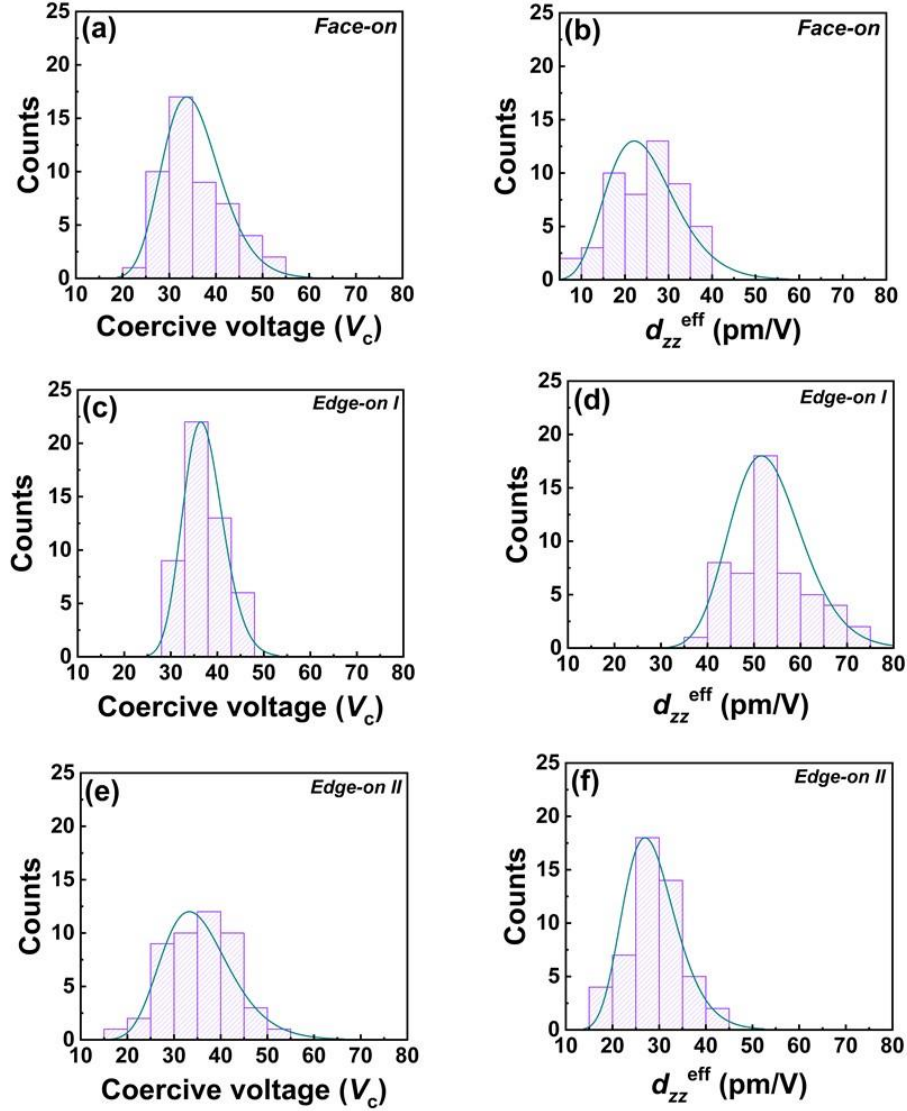
Figure 6. Statistical study of the local switching and electromechanical behaviors in P(VDF-*co*-TrFE) film. Statistical distribution of the (a, c, e) coercive voltages and (b, d, f) piezoelectric coefficients values deduced from the recorded PFM loops, measured on the different types of morphology previously identified for the P(VDF-*co*-TrFE)/BNT/SiO$_2$/Si sample: (a, b) face-on, (c, d) edge-on *I* and (e, f) edge-on *II* domain structures. The curves in cyan represent the log-normal distribution fitting of the various values of V_c and d_{zz}^{eff}.
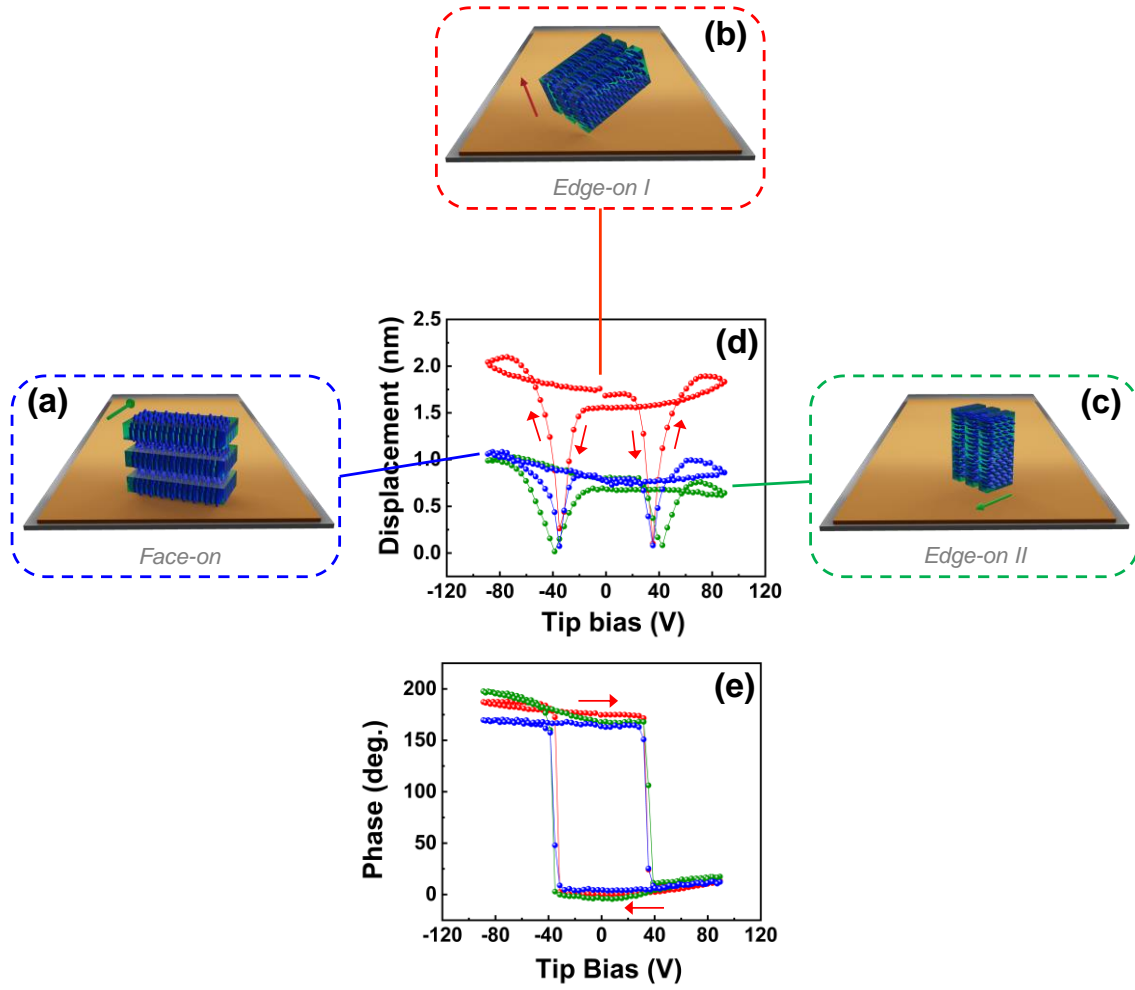
Figure 7. Schematic illustrations of P(VDF-*co*-TrFE) crystalline lamellae associated to PFM loops. (a) Face-on, (b) edge-on *I* and (c) edge-on *II* lamellar structures. Typical (d) amplitude and (e) phase remnant PFM loops recorded on the free surface of the copolymer film and carefully attributed to the type of crystalline structures. Green (in-plane) and red (out-of-plane) arrows in (a-c) represent the polarization vector along the *b*-axis in the various-oriented lamellae with respect to the plane of the substrate.

Table 1. Summarized of the crystalline lamellar structures, average coercive voltages (V_c) and average effective piezoelectric coefficients (d_{zz}^{eff}) determined on the P(VDF-*co*-TrFE) film.

	Face-on	**Edge-on *I***	**Edge-on *II***
V_c **(V)**	33.8	36.4	37.4
d_{zz}^{eff} **(pm/V)**	–30.0	–50.3	–27.1

Graphical abstract
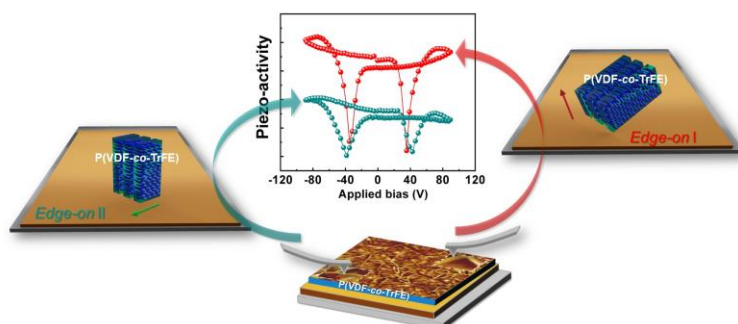
REFERENCES

[1] Asadi K.; Li M.; Stingelin N.; Blom P.W.M.; de Leeuw D.M. Crossbar Memory Array of Organic Bistable Rectifying Diodes for Nonvolatile Data Storage. Applied Physics Letters 97 (2010) 193308. doi:10.1063/1.3508948.

[2] Asadi K.; de Leeuw D.M.; de Boer B.; Blom P.W.M. Organic Non-Volatile Memories from Ferroelectric Phase-Separated Blends. Nature Materials 7 (2008) 547–550. doi:10.1038/nmat2207.

[3] Naber R.C.G.; Asadi K.; Blom P.W.M.; de Leeuw D.M.; B. de Boer B. Organic Nonvolatile Memory Devices Based on Ferroelectricity. Advanced Materials 22 (2010) 933–945. doi:10.1002/adma.200900759.

[4] Naber R.C.G.; Tanase C.; Blom P.W.M.; Gelinck G.H.; Marsman A.W.; Touwslager F.J.; Setayesh S.; de Leeuw D.M. High-Performance Solution-Processed Polymer Ferroelectric Field-Effect Transistors. Nature Materials 4 (2005) 243–248. doi:10.1038/nmat1329.

[5] Baltá Calleja F.J.; González Arche A.; Ezquerra T.A.; Santa Cruz C.; Batallán F.; Frick B.; López Cabarcos E. (1993) Structure and Properties of Ferroelectric Copolymers of Poly(vinylidene fluoride). In: Zachmann H.G. (eds) Structure in Polymers with Special Properties. Advances in Polymer Science, vol 108. Springer, Berlin, Heidelberg. doi:10.1007/3-540-56579-5_1.

[6] Tashiro K.; Takano K.; Kobayashi M.; Chatani Y.; Tadokoro H. Structural Study on Ferroelectric Phase Transition of Vinylidene Fluoride-Trifluoroethylene Copolymers (III) Dependence of Transitional Behavior on VDF Molar Content. Ferroelectrics 57 (1984) 297–326. doi:10.1080/00150198408012770.

[7] Kim J.-H.; Khang D.-Y. High-Performance Needle-Shaped Crystals in Thin and Ultrathin P(VDF-TrFE) Films Formed by Melt Recrystallization. European Polymer Journal 59 (2014) 78–83. doi:10.1016/j.eurpolymj.2014.07.017.

[8] Chang C.; Tran V.H.; Wang J.; Fuh Y.-K. Lin L. Direct-Write Piezoelectric Polymeric Nanogenerator with High Energy Conversion Efficiency. Nano Letters 10 (2010) 726–731. doi:10.1021/nl9040719.

[9] Liu Y.; Weiss D.N.; Li J. Rapid Nanoimprinting and Excellent Piezoresponse of Polymeric Ferroelectric Nanostructures. ACS Nano 4 (2010) 83–90. doi:10.1021/nn901397r.

[10] Martins P.; Lopes A.C.; Lanceros-Mendez S. Electroactive Phases of Poly(vinylidene fluoride): Determination, Processing and Applications. Progress in Polymer Science 39 (2014) 683-706. doi:10.1016/j.progpolymsci.2013.07.006.

[11] Ruan L.; Yao X.; Chang Y.; Zhou L.; Qin G.; Zhang X. Properties and Applications of the β Phase Poly(vinylidene fluoride). Polymers 10 (2018) 228. doi:10.3390/polym10030228.

[12] Park Y.J.; Kang S.J.; Park C.; Kim K.J.; Lee H.S.; Lee M.S.; Chung U.-I.; Park I.J. Irreversible Extinction of Ferroelectric Polarization in P(VDF-TrFE) Thin Films Upon Melting and Recrystallization. Applied Physics Letters 88 (2006) 242908. doi:10.1063/1.2207831.

[13] Katsouras I.; Asadi K.; Li M.; van Driel T.B.; Kjær K.S.; Zhao D.; Lenz T.; Gu Y.; Blom P.W.M.; Damjanovic D.; Nielsen M.M.; de Leeuw D. M. The Negative Piezoelectric Effect of the Ferroelectric Polymer Poly(vinylidene fluoride). Nature Materials 15 (2016) 78–84. doi:10.1038/nmat4423.

[14] Hafner J.; Benaglia S.; Richheimer F.; Teuschel M.; Maier F.J.; Werner A.; Wood S.; Platz D.; Schneider M.; Hradil K.; Castro F.A.; Garcia R.; Schmid U. Multi-Scale Characterisation of a Ferroelectric Polymer Reveals the Emergence of a Morphological Phase Transition Driven by Temperature. Nature Communications 12 (2021) 152. doi:10.1038/s41467-020-20407-6.

[15] Xia W.; Chen Q.; Zhang J.; Wang H.; Cheng Q.; Jiang Y.; Zhu G. Removable Polytetrafluoroethylene Template Based Epitaxy of Ferroelectric Copolymer Thin Films. Applied Surface Science 437 (2018) 209–216. doi:10.1016/j.apsusc.2017.12.126.

[16] Ohigashi H.; Akama S.; Koga K. Lamellar and Bulk Single Crystals Grown in Annealed Films of Vinylidene Fluoride and Trifluoroethylene Copolymers. Japanese Journal of Applied Physics 27 (1988) 2144. doi 10.1143/JJAP.27.2144.

[17] Sharma P.; Wu D.; Poddar S.; Reece T.J.; Ducharme S.; Gruverman A. Orientational Imaging in Polar Polymers by Piezoresponse Force Microscopy. Journal of Applied Physics 110 (2011) 52010. doi:10.1063/1.3623765.

[18] Wu Y.; Li X.; Weng Y.; Hu Z.; Jonas A.M. Orientation of Lamellar Crystals and its Correlation with Switching Behavior in Ferroelectric P(VDF-TrFE) Ultra-Thin Films. Polymer 55 (2014) 970–977. doi:10.1016/j.polymer.2014.01.004.

[19] Liu Y.; Wang Q. Ferroelectric Polymers Exhibiting Negative Longitudinal Piezoelectric Coefficient: Progress and Prospects. Advanced Science 7 (2020) 1902468. doi:10.1002/advs.201902468.

[20] Zhang L.; Li S.; Zhu Z.; Rui G.; Du B.; Chen D.; Huang Y-F.; Zhu L. Recent Progress on Structure Manipulation of Poly(vinylidene fluoride)-Based Ferroelectric Polymers for Enhanced Piezoelectricity and Applications. Advanced Functional Materials (2023) 2301302. doi.org/10.1002/adfm.202301302.

[21] Choi Y.-Y., Sharma P.; Phatak C.; Gosztola D.J.; Liu Y.; Lee J.; Lee B.; Li J. A. Gruverman, S. Ducharme, S. Hong. Enhancement of Local Piezoresponse in Polymer Ferroelectrics via Nanoscale Control of Microstructure. ACS Nano 9 (2015) 1809–1819. doi:10.1021/nn5067232.

[22] Qian J.; Jiang S.; Wang Q.; Zheng S.; Guo S.; Yi C.; Wang J.; Wang X.; Tsukagoshi K.; Shi Y.; Li Y. Unveiling the Piezoelectric Nature of Polar α-Phase P(VDF-TrFE) at Quasi-Two-Dimensional Limit. Scientific Reports 8 (2018) 532. doi:10.1038/s41598-017-18845-2.

[23] Zhang L.; Ducharme S.; Li J. Microimprinting and Ferroelectric Properties of Poly(vinylidene fluoride-trifluoroethylene) Copolymer Films. Applied Physics Letters 91 (2007) 172906. doi:10.1063/1.2800803.

[24] Gaynutdinov R.V.; Mitko S.; Yudin S.G.; Fridkin V.M.; Ducharme S. Polarization Switching at the Nanoscale in Ferroelectric Copolymer Thin Films. Applied Physics Letters 99 (2011) 142904. doi:10.1063/1.3646906.

[25] Liew W.H.; Mirshekarloo W.H.; Chen S.; Yao K.; Tay F.E.H. Nanoconfinement Induced Crystal Orientation and Large Piezoelectric Coefficient in Vertically Aligned P(VDF-TrFE) Nanotube Array. Scientific Reports 5 (2015) 9790. doi:10.1038/srep09790.

[26] Hamieh A.; Ponchel F.; Barrau S.; Remiens D. Synthesis of Lead-Free $(Bi_{0.5}Na_{0.5})TiO_3$ Thin Film by RF Magnetron Sputtering: Impact of Na on the Properties of Film. Ferroelectrics 556 (2020) 79–86. doi:10.1080/00150193.2020.1713345.

[27] Detalle M.; Rémiens D. Chemical and Physical Characterization of $LaNiO_3$ Thin Films Deposited by Sputtering for Top and Bottom Electrodes in Ferroelectric Structure. Journal of Crystal Growth 310 (2008) 3596–3603. doi:10.1016/j.jcrysgro.2008.04.053.

[28] Rodriguez B.J.; Callahan C.; Kalinin S.V.; Proksch R. Dual-Frequency Resonance-Tracking Atomic Force Microscopy. Nanotechnology 18 (2007) 1−6. doi:10.1088/0957-4484/18/47/475504.

[29] Choi J.; Borca C.N.; Dowben P.A.; Bune A.; Poulsen M.; Pebley S.; Adenwalla S.; Ducharme S.; Robertson L.; Fridkin V.M.; Palto S.P.; Petukhova N.N.; Yudin S.G. Phase Transition in the Surface Structure in Copolymer Films of Vinylidene Fluoride (70%) with Trifluoroethylene (30%). Physical Review B 61 (2000) 5760–5770. doi:10.1103/PhysRevB.61.5760.

[30] Bellet-Amalric E.; Legrand J.F. Crystalline Structures and Phase Transition of the Ferroelectric P(VDF-TrFE) Copolymers, a Neutron Diffraction Study. The European Physical Journal B - Condensed Matter and Complex Systems 3 (1998) 225–236. doi:10.1007/s100510050307.

[31] Hu Z.; Tian M.; Nysten B.; Jonas A.M. Regular Arrays of Highly Ordered Ferroelectric Polymer Nanostructures for Non-Volatile Low-Voltage Memories. Nature Materials 8 (2009) 62-67. doi:10.1038/nmat2339.

[32] Roth R.; Koch M.; Schaab J.; Lilienblum M.; Syrowatka F.; Band T.; Thurn-Albrecht T.; Dörr K. Aligning In-Plane Polarization Multiplies Piezoresponse in P(VDF-TrFE) Films on Graphite. New Journal of Physics 20 (2018) 103044. doi:10.1088/1367-2630/aae8b6.

[33] Bargain F.; Panine P.; Domingues Dos Santos F.; Tencé-Girault S. From Solvent-Cast to Annealed and Poled Poly(VDF-co-TrFE) Films: New Insights on the Defective Ferroelectric Phase. Polymer 105 (2016) 144–156. doi:10.1016/j.polymer.2016.10.010.

[34] Spampinato N.; Maiz J.; Portale G.; Maglione M.; Hadziioannou G.; Pavlopoulou E. Enhancing the Ferroelectric Performance of P(VDF-co-TrFE) Through Modulation of Crystallinity and Polymorphism. Polymer. 149 (2018) 66–72. doi:10.1016/j.polymer.2018.06.072.

[35] Gutiérrez-Fernández E.; Rebollar E.; Cui J.; Ezquerra T.A.; Nogales A. Morphology and Ferroelectric Properties of Semiconducting/Ferroelectric Polymer Bilayers. Macromolecules 52 (2019) 7396−7402. doi:10.1021/acs.macromol.9b00859.

[36] Xia W.; Peter C.; Weng J.; Zhang J.; Kliem H.; Jiang Y.; Zhu G. Epitaxy of Ferroelectric P(VDF-TrFE) Films via Removable PTFE Templates and Its Application in

Semiconducting/Ferroelectric Blend Resistive Memory. ACS Appl. Mater. Interfaces 9 (2017) 12130–12137. doi:10.1021/acsami.7b01571.

[37] Chan C.-M.; Li L. Direct Observation of the Growth of Lamellae and Spherulites by AFM. Advances in Polymer Science 188 (2005) 1–41. doi:10.1007/b136971.

[38] López Cabarcos E.; de las Rivas B.; Ezquerra T.A.; Baltá Calleja F.J. Toward Chain Extension in Crystals of Fluorinated Copolymers As Revealed by Real Time Ultra-Small-Angle X-ray Scattering. Macromolecules 31 (1998) 6157-6163. doi.org/10.1021/ma960135i.

[39] Hikosaka M. Unified Theory of Nucleation of Folded-Chain Crystals and Extended-Chain Crystals of Linear-Chain Polymers. Polymer 28 (1987) 1257-1264. doi.org/10.1016/0032-3861(87)90434-4.

[40] Hikosaka M. Unified Theory of Nucleation of Folded-Chain Crystals (FCCs) and Extended-Chain Crystals (ECCs) of Linear-Chain Polymers: 2. Origin of FCC and ECC. Polymer 31 (1990) 458-468. doi.org/10.1016/0032-3861(90)90385-C.

[41] Martínez-Tong D. E.; Soccio M.; García-Gutiérrez M.C.; Nogales A.; Rueda D. R.; Alayo N.; Pérez-Murano F.; Ezquerra T.A. Improving Information Density in Ferroelectric Polymer Films by using Nanoimprinted Gratings. Applied Physics Letters 102 (2013) 191601. doi:10.1063/1.4804427.

[42] Li W.; Zhu Y.; Hua D.; Wang P.; Chen X.; Shen J. Crystalline Morphologies of P(VDF-TrFE) (70/30) Copolymer Films Above Melting Point. Applied Surface Science 254 (2008) 7321–7325. doi:10.1016/j.apsusc.2008.05.339.

[43] Lee J.S.; Prabu A.A.; Kim K.J. Annealing Effect Upon Chain Orientation, Crystalline Morphology, and Polarizability of Ultra-Thin P(VDF-TrFE) Film for Nonvolatile Polymer Memory Device. Polymer 51 (2010) 6319–6333. Doi:10.1016/j.polymer.2010.10.053.

[44] Guo D.; Stolichnov V.; Setter N. Thermally Induced Cooperative Molecular Reorientation and Nanoscale Polarization Switching Behaviors of Ultrathin Poly(vinylidene fluoride-trifluoroethylene) Films. Journal of Physical Chemistry B 115 (2011) 13455–13466. doi:10.1021/jp2061442.

[45] Hahm S.-W.; Khang D.-Y. Crystallization and Microstructure-Dependent Elastic Moduli of Ferroelectric P(VDF–TrFE) Thin Films. Soft Matter. 6 (2010) 5802–5806. doi:10.1039/C0SM00350F.

[46] Sharma P.; Reece T.J.; Ducharme S.; Gruverman A. High-Resolution Studies of Domain Switching Behavior in Nanostructured Ferroelectric Polymers. Nano Letters 11 (2011) 1970–1975. doi:10.1021/nl200221z.

[47] Guo M.; Jiang J.; Qian J.; Liu C.; Ma J.; Nan C.-W.; Shen Y. Flexible Robust and High-Density FeRAM from Array of Organic Ferroelectric Nano-Lamellae by Self-Assembly. Advanced Science 6 (2019) 1801931. doi:10.1002/advs.201801931.

[48] Hu W.J.; Juo D.-M.; You L; Wang J.; Chen Y.-C.; Chu Y.-H.; Wu T. Universal Ferroelectric Switching Dynamics of Vinylidene Fluoride-trifluoroethylene Copolymer Films. Scientific Reports 4 (2014) 4772. doi: 10.1038/srep04772.

[49] Furukawa T. Ferroelectric Properties of Vinylidene Fluoride Copolymers. Ferroelectrics 18 (1988) 143-211. doi:10.1080/01411598908206863.

[50] Fridkin V.M.; S. Ducharme. General Features of the Intrinsic Ferroelectric Coercive Field. Physics of the Solid State 43 (2001) 1320–1324. doi:10.1134/1.1386472.

[51] Li A.; Ge C.; Lü P. Preparation of Perovskite Conductive $LaNiO_3$ Films by Metalorganic Decomposition. Applied Physics Letters 68 (1996) 1347. doi:10.1063/1.115930.

[52] Lau K.; Liu Y.; Chen H.; Withers R.L. Effect of Annealing Temperature on the Morphology and Piezoresponse Characterisation of Poly(vinylidene fluoride-trifluoroethylene) Films via Scanning Probe Microscopy. Advances in Condensed Matter Physics 2013 (2013) 5. doi:10.1155/2013/435938.